Tribology Letters (2022) 70:58
https://doi.org/10.1007/s11249-022-01596-1

TRIBOLOGY METHODS

Enhancement of a Tribometer Device Dedicated to Quasi-Static Friction Conditions Under High Pressure

R. Massion[1,2] · C. Franoux[1] · C. Dureau[1,2] · J. Vincent[1] · L. Faure[1,2] · S. Philippon[2,3]

Received: 13 January 2022 / Accepted: 1 April 2022 / Published online: 29 April 2022

Abstract

A new version of an original tribometer has been developed to measure friction coefficients under high pressures in quasi-static conditions. This study describes the design of the new tribometer device and aims to cancel any defects noted in the previous release. This configuration, combined with the improvement of the tribometer's guidance stiffness, increases the sliding distance from 1 to 30 mm while keeping a normal pressure accuracy and creates possible pressure tests ranging from 500 to 2000 MPa. In order to validate the assembly and to simulate testing conditions in severe plastic deformation processes of metals, two tribo-pairs consisting of interstitial free steels and aluminum alloy (Al 1050) samples sliding on 45NiCrMo16 steel matrices were tested. New results on the friction coefficient evolution throughout a sliding length of 10 mm were noted and all tests revealed good reproducibility for the whole pressure range.

Keywords Dry friction · High pressure · Severe plastic deformation

1 Introduction

Tribological aspects occur in most part of material forming processes, whether or not desired. They play a leading role in forces to apply or even in the final roughness of a workpiece depending on contact pressure [1], sliding velocity or length [2].

Severe Plastic Deformation (SPD) techniques are generally used to produce grain refinement in metals in order to increase the yield strength or to perform surface treatments for instance. In addition, observations show that some materials produced with SPD processes under specific conditions exhibit improved tribological features. Many studies show a real enhancement of friction properties between two materials rubbing against each other involving one obtained through the SPD process [3]. Indeed, the use of a material produced via an SPD technique such as High Pressure Torsion (HPT) for instance, leads to an overall increase in wear resistance [4] and a decrease in friction coefficients [5]. Chegini and Shaeri [6] and Abd El Aal et al. [7] reported similar observations by increasing the number of Equal Channel Angular Extrusion (ECAP) passes, respectively, on Al-7075 alloy and on different Al–Cu alloys.

Nevertheless, SPD processes are also affected by contact conditions. In the most popular of them such as ECAP HPT, friction between sample and dies or anvils significantly influences the back-pressure value and the plastic strain distribution in the sample [8, 9]. In a single pass of HPT, the hydrostatic pressure generates an extremely large amount of strain, higher than in other SPD processes, which leads to an average grain size which is smaller than those produced by ECAP [10] and to strengthening mechanisms [11]. Most SPD technique are conducted in static mode but in order to obtain different materials properties, some SPD processes involve a dynamic mode. Verleysen et al. [12] for example studied a new dynamic HPT technique inspired by torsional split Hopkinson bar (TSHB) setups.

Numerical studies performed on the ECAP process pointed the sensitivity of this SPD technique on friction

✉ R. Massion
roxane.massion@univ-lorraine.fr

1 LEM3 Laboratoire d'Etude des Microstructures et de Mécanique des Matériaux, Université de Lorraine, CNRS UMR 7239, Arts et Métiers ParisTech, 7 rue Félix Savart, 57070 Metz, France

2 Laboratory of Excellence on Design of Alloy Metals for Low-mAss Structures, 'DAMAS', Université de Lorraine, 7 rue Félix Savart, 57070 Metz Cedex, France

3 LEM3 Laboratoire d'Etude des Microstructures et de Mécanique des Matériaux, Université de Lorraine, CNRS UMR 7239, Ecole Nationale d'Ingénieurs de Metz, 1 route d'Ars Laquenexy, 57070 Metz, France

and the strong influence to this phenomenon on the distribution of stresses in the die corner [13] and on the billet for aluminum alloy [14]. However, despite these observations, experimental characterization of dry friction occurring during SPD processes is rarely investigated. As a consequence, there is a clear need to characterize the dry friction coefficient in representative SPD working conditions, i.e., for a couple of materials for which a sample is confined under high hydrostatic pressure, and considering a low sliding velocity for different contact lengths and various degrees of initial roughness of the matrices (die and anvil).

Designing an experimental device with all these characteristics involves many difficulties to overcome and some studies were carried out in this regard. In order to apply a high hydrostatic pressure [15], techniques to confine a sample have been adapted for the investigation of friction [16] between a couple of materials made up of aggregate material and steel for low sliding velocity [17]. Xinghua et al. [18] also developed an experimental method to characterize friction properties of sheet metal under high contact pressure. Unfortunately, the pressure in those studies does not exceed 100 MPa. With a view to studying IF steel sample rubbing between two 45NiCrMo16 steel matrices, Pougis et al. [19] proposed an original device specially designed to meet SPD specifications of their own ECAP and HTP setups to investigate dry friction evolution under high pressures ranging from 200 MPa to 1 GPa and for low sliding velocities of a few centimeter per minute with various initial surface roughness of the matrices.

The goal of this study is to present an updated version of this original device considering that the first experimental results highlighted some limitations of this tribometer. Improvements were made to this tribometer not only to make it better suited to the SPD processes such as ECAP or HPT but also to ensure better reproducibility of the measurements. The initial sliding distance was extended to 10 mm under higher apparent normal pressures (up to 2 GPa) with a view to obtaining dry friction coefficient values representative of the operating conditions in SPD processes. A few tests for a couple of steel materials were first performed to demonstrate the validity of changes and provide new results for the highest normal pressures (2 GPa).

2 Material and Methods

2.1 The Pougis et al. Configuration

The design and the description of the operation of the device are precisely reported in the article published by Pougis et al. [19]. Figure 1 describes the working principle of this tribometer that consists of pressing a sliding cylindrical specimen constrained in a bore machined in the plunger between two fixed matrices. Then, the sliding is induced by applying a force on the plunger using a standard testing machine.

Nevertheless, although its efficiency has been generally satisfactory some issues emerged during its use and were notified. The most representative are reported here. In Pougis et al.'s configuration, the apparent normal pressure was applied by two sets of instrumented screws-nut system (1–2) located on both sides of the investigated tribo-pair of materials. Each set is manually and independently driven, leading

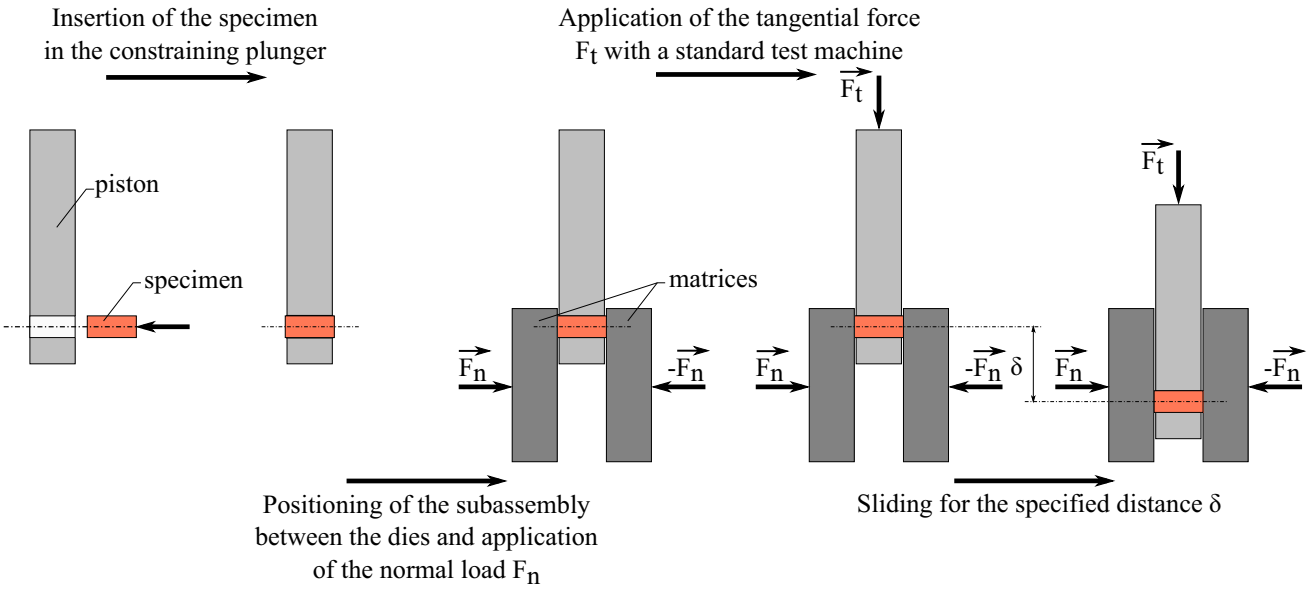

Fig. 1 Working principle of the tribometer

to a possible dissymmetric loading (Fig. 2). Thus, the combination of the standard screw-thread value and the short distance δ (see Fig. 2) makes the precise adjustment of the normal load very challenging. In addition, the parallelism between the two jaws (3) during the loading phase is also quite difficult to ensure easily. This requirement is mandatory to impose uniform pressure onto the sample (6) and to avoid any undesirable contact between the moving plunger (4) and the matrices (5). Another angular misalignment can be also noted between the two jaws in the perpendicular direction (Fig. 2). It mainly depends on the dimension γ, which is the position of the sample throughout the test with respect to the loading plane defined by the two axes of the screws. The farther the sample is from this plane, the greater the misalignment. Consequently, the friction length was limited to a short distance (maximum value of 1 mm) to ensure the stability of the initial experimental parameters all along the friction test.

The maximum normal pressure (manually applied on the sample) mostly depends on the mechanical strength of the screw-nut assemblies allowing an apparent normal pressure close to 1 GPa. Considering that the manually applied forces on the two screw-nut assemblies must be strictly identical and considering what the necessary operating clearances need to be, this inevitably leads to angular deviations between the jaws' surfaces. As a result, consistency and symmetry of loading at the sliding interfaces cannot be fully guaranteed with this configuration. Pougis et al. observed a drop in the normal load from 0.2 to 36.5% throughout the test depending on the normal pressure that was initially applied. The strongest variations which were observed for low pressures can be mainly explained by a lack of guidance solution for the mobile parts as well as by the device stiffness weakness, which means that the higher the applied pressure, the stiffer the tribometer device. Moreover, to avoid any parasite contact between the surfaces of the matrices and the plunger that may change the friction conditions at the interface, the apparent normal pressure remains limited to 1 GPa.

Although the previous version of the tribometer device has provided first results highlighting the influence of main parameters on dry friction, the working conditions are limited by the tribometer device design itself. These values of the friction path length and the apparent pressure are too far from those observed in SPD processes where the confined sample slides from a few millimeters to several centimeters in length under an apparent normal pressure up to 2 GPa. The new architecture developed for the new tribometer notably aims to eradicate most of these issues while improving its ability to perform dry friction tests close to the conditions of SPD processes, with greater accuracy and repeatability.

2.2 Architecture of the New Tribometer Device

While keeping the general working principle, the design of the new tribometer device aims to cancel any defects noted in the previous release and to meet several major requirements where a confined cylindrical sample slides between two massive jaws supporting the matrices.

The lack of stiffness and the excessive operating clearances of the mobile jaws with the fixed frame are strongly reconsidered. In this new version (Fig. 3), the guidance of the mobile jaw (7) is now ensured by three massive circular columns (2) rigidly fixed to the structure (6). The one (2)

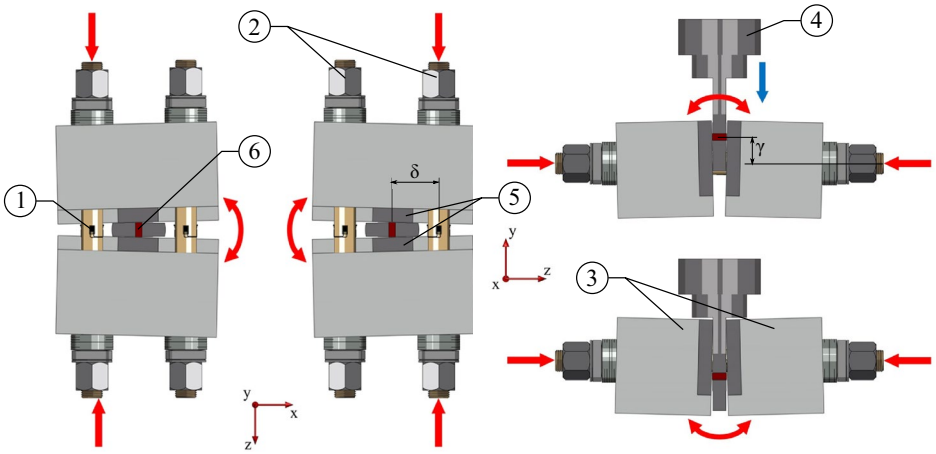

Fig. 2 Pougis's configuration: illustration of the dissymmetric phenomenon and of the angular misalignment loading phenomenon

N°	Part	N°	Part
1	Screw with strain gauges	4	Plunger
2	Nuts	5	Matrices
3	Jaws	6	Sample

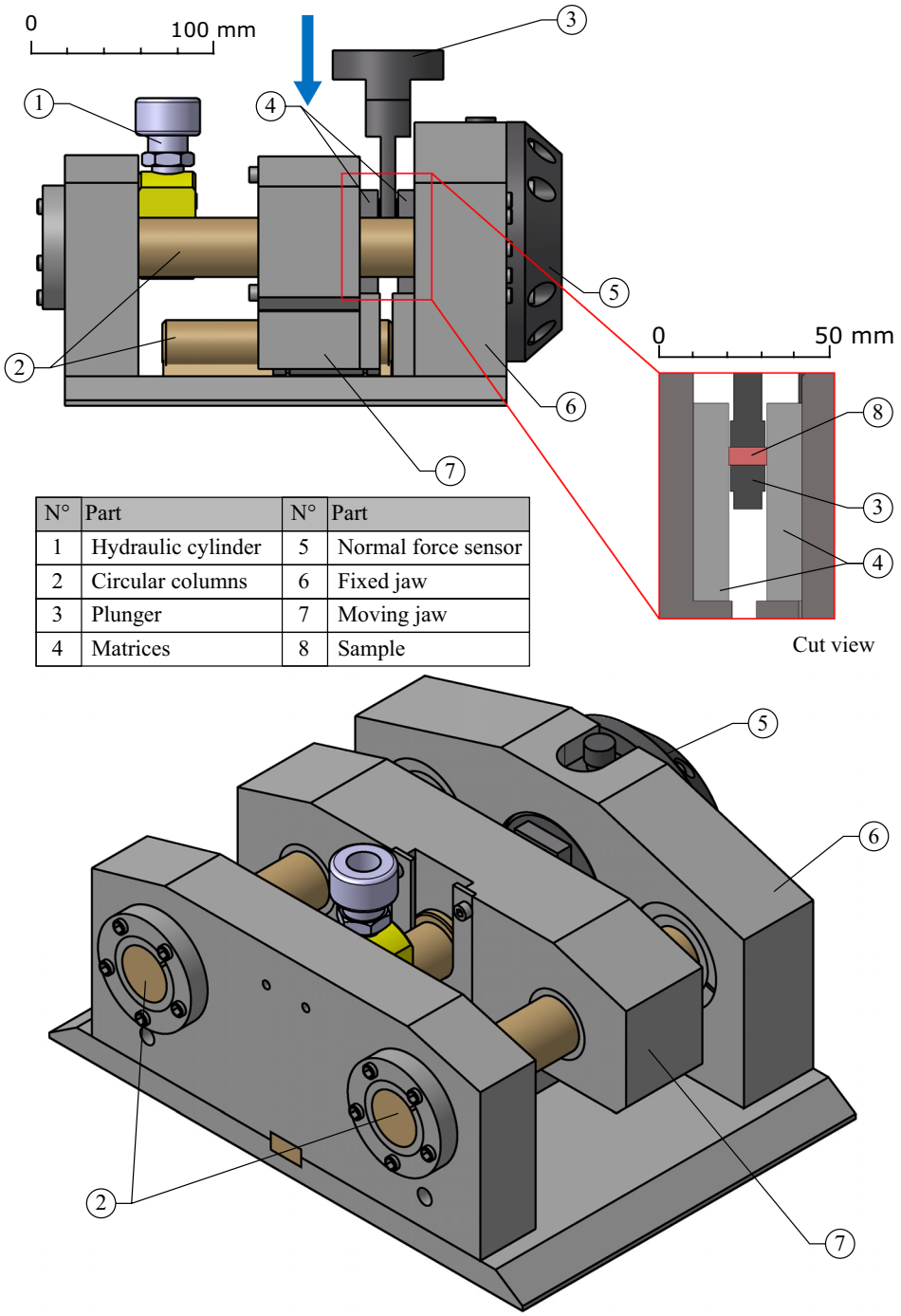

N°	Part	N°	Part
1	Hydraulic cylinder	5	Normal force sensor
2	Circular columns	6	Fixed jaw
3	Plunger	7	Moving jaw
4	Matrices	8	Sample

Fig. 3 CAD view of the new tribometer device

underneath the mobile jaw (7) does not contribute to guidance but contributes to increasing the stiffness of the structure by minimizing the bending displacements. This solution enables the mobile part to shift keeping the parallelism of the jaws surfaces while avoiding angular deflections. This technical solution is obviously mechanically constraining but it is often used in other engineering fields (e.g., with universal testing machine) in order to meet these geometrical requirements.

As previously stated, owing to the difficulty of manually balancing the compressive forces on each side of the mobile jaws, the two independent screw-nut assemblies did not make it possible to apply a strictly uniform normal pressure at the sliding interfaces. This former configuration is now substituted by a single hydraulic actuator located on the loading axis of the tribometer and sample. The major consequence of these changes is easily controllable pressure (Fig. 4).

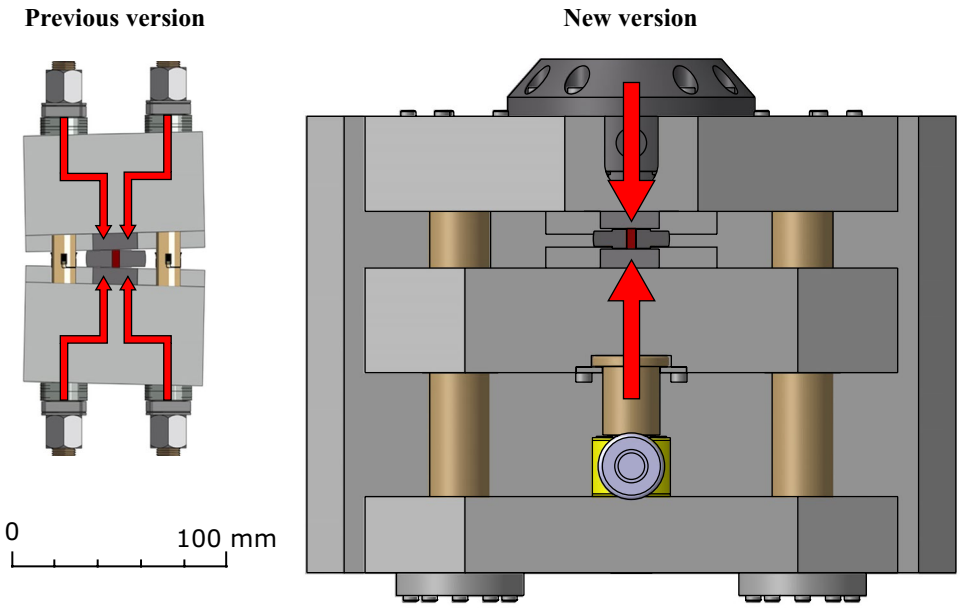

Fig. 4 Comparison between the previous and the new tribometer device

Previously, the apparent normal pressure was checked throughout the friction path by means of strain gauges glued on each screw-nut system. This measurement procedure has now been improved in a robust way by means of a high capacity force sensor positioned close to the specimen which transmits the normal force signal to a DEWETRON signal conditioner (DEWE-3020 with DAQP-STG conditioner). This configuration, combined with the improvement in guidance stiffness, increases the sliding distance from 1 to 30 mm while keeping normal pressure accuracy. All the characteristics of the original tribometer device are listed in Table 1. Test results on IF steel and Al alloys performed with this new device are presented in the following section.

3 Results and Discussion

3.1 Comparison Between the Two Setups

With a view to comparing the two existing tribometer devices, several tests have been performed with the same experimental parameters. The matrices are made of ground 45NiCrMo16 steel (EN10027, AISI 6F7), heat treated to achieve 440 HV and the samples are IF steel (whose composition in weight percentage is: 0.0018C, 0.095 Mn, 0.026 Cu, 0.023 Cr, 0.06 Al, 0.046 Ti, Fe balance). The samples dimensions are 5 mm in diameter and 10.8 mm in length (sample surfaces polished with a 2400 grade silicon paper). All tests were carried out at room temperature (20 °C) in dry conditions. The tribometer was put on a tensile-compression testing machine. The axe of the mandrel was aligned with the one of the plungers of the tribometer. The displacement of the plunger was driven by the mandrel of the testing machine at 5 mm/min. Those tests are called displacement-controlled tests (DC) and they aim to determine the kinetic friction coefficient μ_K.

A typical recording of the measured forces evolution during a test is presented in Fig. 5. By the means of the hydraulic actuator, the normal force acting on the specimen is initially set to 20 000 N corresponding to a pressure at the sample surface close to 1 GPa (for a 5 mm sample diameter). Once the test is started and after a short transient period a continuous drop of about 20% of this normal force is observed over the duration of the test. This can be explained by the rubbing and the consecutive wear of the specimen against the matrices throughout the 10 mm displacement.

Table 1 Characteristics of the new tribometer device

Sliding length	Up to 30 mm	
Pressure	Up to 2 GPa (5 mm diameter specimen)	
Normal force	< 40 kN	
Tangential force	Depends on the load cell	
Speed	Tensile-compression testing machine	0–10 mm/s
	Dynamic tensile-compression testing machine	Up to 10 m/s
	Drop weight impact testers	Up to 16 m/s

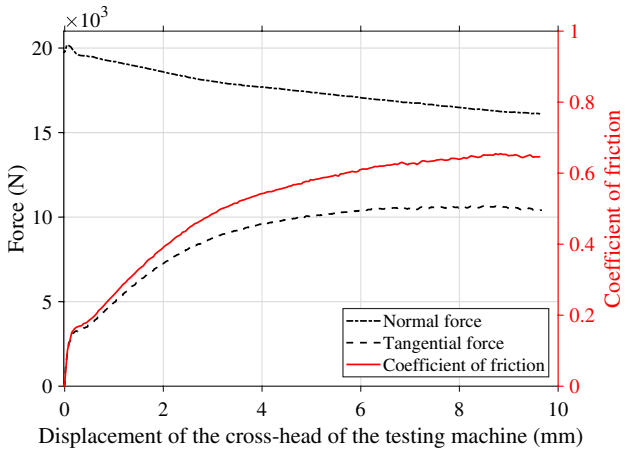

Fig. 5 Typical recorded forces and calculated coefficient of friction with respect to the cross-head displacement of the testing machine (#IF-1)

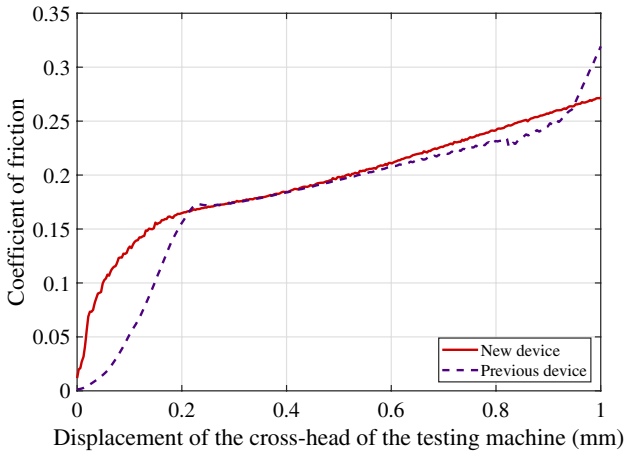

Fig. 7 Value of the coefficient of friction with respect to the displacement for both the previous device and the new device

The constant velocity (5 mm/min) of the cross-head of the testing machine results in a steady increase wear of the specimen. This leads to a reduction in length of the specimen and consequently a drop of the applied normal force (considering the single hydraulic actuator acting on the mobile jaw is not being controllable during the test). Despite this, the tangential force and the coefficient of friction achieve a stable phase from 6 to 10 mm.

Figure 6 shows the results of the three tests carried out on the new tribometer device. These three tests with a sliding length of 10 mm indicated a steady state of the coefficient of friction from 8 to 10 mm with an average of 0.62. To compare these results with the previous study an average curve of those three tests on a sliding length of 1 mm has been calculated and represented in Fig. 7 with the friction coefficient evolution of the previous device. Figure 7 shows a similar evolution of the coefficient of friction on 1 mm sliding length for the new and the previous device. Furthermore, the stabilizing period at the beginning of the test is approximately 25% shorter for the new tribometer device (approximately 0.2 mm and 0.15 mm for the previous and the new device, respectively). This can be explained by a greater adjustment and precision of the different guiding parts of the new tribometer.

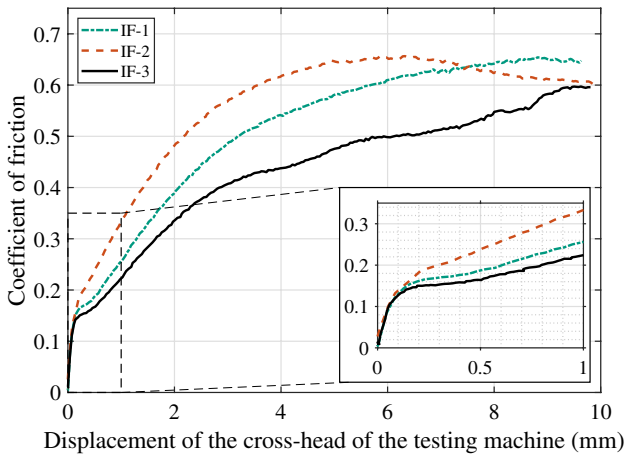

Fig. 6 Evolution of the friction coefficient for IF steel under 1000 MPa at a sliding speed of 5 mm/min

3.2 Application to ECAP

In order to extend our results, a study on a 1050 aluminum alloy, a material commonly used in the ECAP process, has been conducted. In fact, the new tribometer in a tension–compression machine and DC-test setup matches the ECAP process where the sample rubs against the canal. Since it is difficult to find data about the coefficient of friction between the sample and the canal, this tribometer device can estimate it for the first millimeters at the beginning of the ECAP process.

The sample dimensions and the matrices material (ground 45NiCrMo16 steel) remained unchanged at a sliding distance of 10 mm and at a sliding velocity of 5 mm/min. Experimental measurements of the coefficient of friction were performed at room temperature, in dry conditions. Two tests were run for repeatability for each chosen pressure level (500, 1000 and 2000 MPa).

Figure 8 reveals good reproducibility of the results for all the tested pressures even for the highest pressure of 2 GPa. For each pressure level the coefficient curve is divided into a transient zone and a plateau. As the pressure increases, the stabilized coefficient of friction decreases. It can also be noticed that using the new device, the higher the pressure, the shorter the transient zone.

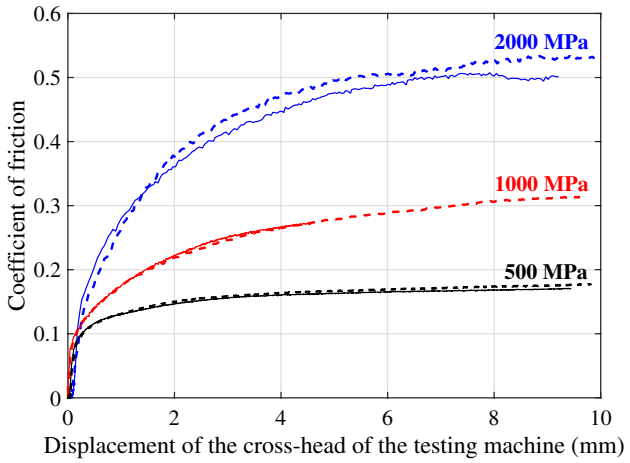

Fig. 8 Calculated curves of coefficient of friction under different contact pressures for 1050 aluminum alloy at a sliding speed of 5 mm/min (— test 1; --- test 2)

4 Conclusions

An enhancement of the previous experimental setup from Pougis et al. has been developed. The purpose of this setup is to measure the friction coefficient under high pressure including in severe plastic deformation process conditions (quasi-static, dry sliding). The couple of materials chosen to compare the two existing tribometers were 45NiCrMo16 (grounded matrices) and IF Steel (sample). A new sample made of Al alloys with a range of pressure between 500 MPa and 2 GPa also have been investigated. The results of the present investigations lead to the main following conclusions:

- In the new setup the guidance of the mobile jaw is now possible. This solves the lack of stiffness affecting the previous setup. With this new solution, the displacement of the mobile part is made possible while keeping the surfaces of the jaws parallel and avoiding angular deflections.
- The previous loading device was an assembly of two independent screw-nuts where applying a strictly uniform normal pressure at the sliding interfaces was not possible. This assembly was substituted by a unique hydraulic cylinder, which resulted in distributing normal pressure onto the sample more evenly and controlling it more easily.
- The sliding length of the new setup can go up to 20 mm and reveals good reproducibility of the results for all the tested pressures. It also confirms the previously suggested fact that the tribometer is more easily controllable at high pressures.
- The kinematic friction coefficient μ_K depends on the sliding length and seems to become steady between 10 and 15 mm. Further investigations will confirm this point.

Funding The authors have not disclosed any funding.

Declarations

Conflict of interest The authors have not disclosed any competing interests.

References

1. Lim, S.C., Ashby, M.F., Brunton, J.H.: The effects of sliding conditions on the dry friction of metals. Acta Metall. **37**, 767–772 (1989). https://doi.org/10.1016/0001-6160(89)90003-5
2. Tamai, Y., Inazumi, T., Manabe, K.: Journal of Materials Processing Technology FE forming analysis with nonlinear friction coefficient model considering contact pressure, sliding velocity and sliding length. J. Mater. Process. Tech. **227**, 161–168 (2016). https://doi.org/10.1016/j.jmatprotec.2015.08.023
3. Li, W.L., Tao, N.R., Han, Z., Lu, K.: Comparisons of dry sliding tribological behaviors between coarse-grained and nanocrystalline copper. Wear **274–275**, 306–312 (2012). https://doi.org/10.1016/j.wear.2011.09.010
4. Ibrahim, M., El, A., Kim, H.S.: Tribology International Effect of the fabrication method on the wear properties of copper silicon carbide composites. Tribiol. Int. **128**, 140–154 (2018). https://doi.org/10.1016/j.triboint.2018.07.024
5. Ibrahim, M., El, A., Seop, H.: Wear properties of high pressure torsion processed ultrafine grained Al–7 % Si alloy. Mater. Des. **53**, 373–382 (2014). https://doi.org/10.1016/j.matdes.2013.07.045
6. Chegini, M., Hossein, M.: Materials Characterization Effect of equal channel angular pressing on the mechanical and tribological behavior of Al–Zn–Mg–Cu alloy. Mater. Charact. **140**, 147–161 (2018). https://doi.org/10.1016/j.matchar.2018.03.045
7. Ibrahim, M., El, A., El, N., Shehata, F.A., Abd, M., Hameed, E., et al.: Wear properties of ECAP-processed ultrafine grained Al–Cu alloys. Mater. Sci. Eng. A **527**, 3726–3732 (2010). https://doi.org/10.1016/j.msea.2010.03.057
8. Edalati, K., Horita, Z.: Materials Science & Engineering A Review article A review on high-pressure torsion (HPT) from 1935 to 1988. Mater. Sci. Eng. A **652**, 325–352 (2016). https://doi.org/10.1016/j.msea.2015.11.074
9. Kamrani, M., Levitas, V.I., Feng, B.: Materials Science & Engineering A FEM simulation of large deformation of copper in the quasi-constrain high-pressure-torsion setup. Mater. Sci. Eng. A **705**, 219–230 (2017). https://doi.org/10.1016/j.msea.2017.08.078
10. Zhilyaev, A.P.: Orientation imaging microscopy of ultrafine-grained nickel. Scr. Mater. **46**, 575–580 (2002)
11. Lanjewar, H., Kestens, L.A.I., Verleysen, P.: Damage and strengthening mechanisms in severely deformed commercially pure aluminum: experiments and modeling. Mater. Sci. Eng. A **800**, 140224 (2021). https://doi.org/10.1016/j.msea.2020.140224
12. Verleysen, P., Lanjewar, H.: Dynamic high pressure torsion: a novel technique for dynamic severe plastic deformation. J. Mater. Process. Technol. **276**, 116393 (2020). https://doi.org/10.1016/j.jmatprotec.2019.116393
13. Deng, G.Y., Lu, C., Tieu, A.K., Su, L.H., Huynh, N.N., Liu, X.H.: Crystal plasticity investigation of friction effect on texture evolution of Al single crystal during ECAP. J. Mater. Sci. **45**, 4711–4717 (2010). https://doi.org/10.1007/s10853-010-4674-2
14. Kumar, P., Panda, S.S.: Numerical simulation of Al1070 alloy through hybrid SPD process. Int. J. Adv. Manuf. Technol. (2016). https://doi.org/10.1007/s00170-016-9768-9

15. Forquin, P.: An experimental method of measuring the confined compression strength of geomaterials. Int. J. Solids Struct. **44**, 4291–4317 (2007). https://doi.org/10.1016/j.ijsolstr.2006.11.022
16. Karinski, Y.S., Yankelevsky, D.Z., Zhutovsky, S., Feldgun, V.R.: Uniaxial confined compression tests of cementitious materials. Constr. Build. Mater. **153**, 247–260 (2017). https://doi.org/10.1016/j.conbuildmat.2017.07.010
17. Durand, B., Delvare, F., Bailly, P., Picart, D.: International Journal of Solids and Structures Identification of the friction under high pressure between an aggregate material and steel: experimental and modelling aspects. Int. J. Solids Struct. **50**, 4108–4117 (2013). https://doi.org/10.1016/j.ijsolstr.2013.08.021
18. Lai, X., Xia, Y., Wu, X., Zhou, Q.: An experimental method for characterizing friction properties of sheet metal under high contact pressure. Wear **289**, 82–94 (2012). https://doi.org/10.1016/j.wear.2012.04.011
19. Pougis, A., Philippon, S., Massion, R., Faure, L., Fundenberger, J.J., Toth, L.S.: Dry friction of steel under high pressure in quasi-static conditions. Tribol. Int. **67**, 27–35 (2013). https://doi.org/10.1016/j.triboint.2013.06.018